Associations between the Slowdown in North Atlantic Tropical-Cyclone Translation Speed and Intensifying Storm Precipitation

Kyra McCreery

North Shore High School

450 Glen Cove. Ave, Glen Head, NY 11545

November 2019

Acknowledgements

I would like to express my gratitude to Dr. Upmanu Lall, Director of the Columbia Water Center at Columbia University, for providing mentorship and guidance during all stages of this research. I would also like to thank Dr. Jennifer Nakamura of the Lamont-Doherty Earth Observatory at Columbia University for generously providing data for use in the analyses. My thanks are also due to Dr. Yochanan Kushnir of the Lamont-Doherty Earth Observatory for his valuable feedback at various stages of the research process.

Introduction

A. Relevant Background

North Atlantic hurricanes are catastrophic natural phenomena with the potential to destroy and destabilize coastal communities, economies, and environments. In recent decades, scientists and government institutions alike have observed increasingly severe hurricane impacts often attributed to anthropogenic (human-induced) warming (Kossin, 2018). Although the intensifying strength and frequency of North Atlantic hurricanes is well-documented in the media and in scientific literature, a comprehensive understanding of the complex and often contradictory links between anthropogenic warming and hurricanes in the Atlantic basin continues to elude the scientific community.

The standard explanation for the increasing severity of North Atlantic storms is that an increase in global sea surface temperature fuels stronger and more destructive hurricanes that advect increased oceanic heat through convection. While this statement certainly accounts for a portion of the changes to North Atlantic hurricane activity observed over the last few decades, the physical mechanisms impacted by shifting climate patterns are far more complex and nuanced, often impacting hurricanes in conflicting and inconsistent ways.

This study aims to examine one specific aspect of the link between anthropogenic warming and North Atlantic hurricane activity: the decline in hurricane translation speed and the subsequent increase in storm precipitation accumulation and associated flooding. Prior research in this realm has identified a reduction in the translation speed of North Atlantic tropical cyclones since 1950, but the connections between this translation speed reduction and other metrics of hurricane activity, such as rainfall accumulation at landfall, have not been readily studied. In a study conducted by Kossin in 2018, a proposed relationship between anthropogenic warming and a quantifiable slowdown in North Atlantic tropical cyclone translation speed is examined, but the primarily objective of the research is an investigation of the possible atmospheric causes underlying the slowdown rather than an analysis of the impacts of this slowdown on hurricane intensity and precipitation. As earlier research by Coumou *et al.* in 2015 stipulates, the physical mechanism linked to the global slowdown is the weakening of the summer prevailing wind circulation in the Northern hemisphere, a phenomenon directly linked to the increase in global temperatures associated with anthropogenic warming. Coumou *et al*. determined that rapid global warming influences the mid-latitude prevailing circulation by reducing the poleward temperature gradient, a hypothesis that initially garnered support in the 1970s and recently re-emerged at the forefront of scientific literature (Screen and Simmons, 2014). As human-induced warming heats the globe, the mid-latitude circulation that typically steers hurricanes towards the contiguous US and then up the coast becomes significantly reduced in strength, causing TCs to stagnate in one region for extended periods before continuing on their paths. The reduced speed of these TCs may intensity their impacts in a plethora of interconnected ways, increasing the amount of precipitation recorded by coastal regions, exacerbating pre-existing flooding risks, and compounding potentially catastrophic storm surge (Kossin 2018). An additional compounding factor is the increased moisture capacity of the atmosphere in a warming world, a variable that may heighten the already severe impacts of these lingering TCs on vulnerable regions.

This study expands upon the findings of prior research in two crucial ways. First, an expanded dataset of years extending from 1851-2016 is utilized to assess and quantify the global slowdown in translation speed based on the trajectories of 1,857 storms in the North Atlantic basin. This study then further differentiates from prior research by taking a spatial approach and investigating the characterization of spatial patterns in the location of the slowest component of North Atlantic tropical cyclone tracks. A number of distinct statistical analyses, including a k-means clustering analysis of translation speeds and a k-nearest neighbor outlier detection analysis, are employed to identify key trends and patterns in the nature of tropical cyclone translation speed over time. Shifting patterns in not only the speed of hurricane movement but the spatial distribution of tropical cyclones defined by unusually slow speeds can offer critical insight into the influence of anthropogenic warming on the location of stalling storms. An understanding of this relationship could inform tropical cyclone model forecasts and seasonal hurricane simulations responsible for the prediction and modeling of hurricane development based on key atmospheric factors.

Based on the results of the translation speed analysis, an examination of the rainfall associated with all storms contained within the dataset that make landfall in the contiguous US is then undertaken to assess changes in both the extent and distribution of tropical cyclone rain fields. Although this component of the analysis is limited by the availability of accurate rain field data, a preliminary analysis is conducted according to the described procedure. The full methodology developed for the completion of this examination is then detailed for future analyses. The precipitation accumulation rate of all storms within the dataset on their date of landfall is initially examined through a linear regression analysis undertaken to uncover preliminary trends in rainfall intensity over time. The next component of the precipitation analysis involves a two-part study comprised of a visual observation of synoptic weather maps illustrating both the rain fields and geopotential height anomalies associated with each landfalling storm on the dates preceding and following the storm, following by a comprehensive hierarchal clustering evaluation of the spatial characterization of the tropical cyclone rain fields at landfall. The research culminates in a discussion of the findings of both analyses in the context of anthropogenic warming and statistical hurricane modeling.

B. Project Goals

1. Research Questions

Over the course of this study, two major questions are emphasized. These questions are summarized below:

I) How has the translation speed of North Atlantic hurricanes changed over time?

II) How has the slowdown in North Atlantic hurricane translation speed impacted the extent and spatial distribution of TC rain fields?

2. Hypotheses

Two distinct hypotheses are formulated in response to the research questions stipulated above. These hypotheses do not encompass the entirety of the analyses conducted as part of this investigation, but they respond directly to the key research questions indicated above. These hypotheses are outlined below.

I) If the mid-latitude planetary circulation is weakened due to anthropogenic warming, and I examine the minimum translation speed of 1,857 tropical storms between 1851-2016, then this minimum translation speed will decline over this period.

II) If the slowdown in translation speed increases the duration of time that coastal regions are exposed to extreme precipitation, and I examine the precipitation accumulation rate associated with 185 landfalling hurricanes between 1950-2011, then the precipitation accumulation rate will increase during this period.

Methods

A. Data

1. Hurricane Position Data

The tropical cyclone position data utilized in this study is derived from the HURDAT2 dataset, a comprehensive repository of storm track data maintained by the National Hurricane Center (NHC). The HURDAT2 dataset contains updated information on storm trajectory and internal storm conditions like pressure and wind speed at every measured interval throughout the hurricane's track. The hurricane dataset modified for this analysis contains information on the complete lifecycle of 1,857 tropical cyclones classified as at least a tropical depression for one or more position observations. The dataset contains a record of the latitude and longitude of each storm at six-hour intervals, along with the date of the observation and the wind speed of the storm if available. The HURDAT2 record is considered less accurate pre-1944, the year that reconnaissance aircraft flights began to reliably document hurricane activity in the North Atlantic (Villarini *et. al* 2011). Missing values observed in the data prior to the mid-1900s can be attributed to inconsistencies and inaccuracies in the HURDAT2 dataset prior to the implementation of flight-based data collection.

2. *Precipitation Datasets*

Two separate precipitation datasets of varying resolutions are utilized to conduct the rainfall component of the analysis. To produce the rain field synoptic maps for the dates of hurricane landfall, an appended dataset modified to combine the CPC Retro Global Unified Gauge-Based Analysis of Daily Precipitation and CPC Realtime Global Unified Gauge-Based Analysis of Daily Precipitation (Chen *et al*, 2008) is constructed. This dataset encompasses the interpolated daily precipitation data for the entire contiguous US at 0.5 x 0.5-degree resolution. To improve experimental accuracy and obtain more authentic conclusions during the second component of the precipitation analysis, a spatial precipitation dataset with a finer resolution is selected. The Livneh daily CONUS near-surface gridded meteorological and derived hydrometeorological data for precipitation accumulation, available at an extremely precise 1/16-degree resolution from 1911-2011, is selected for the hierarchal clustering component of the analysis. The Livneh dataset interpolates the daily precipitation accumulation across the entirety of the contiguous US, providing an accurate reconstruction of the precipitation conditions associated with each landfalling storm at its time of landfall.

2. Geopotential Height Anomalies Dataset

As part of the investigation into the links between the slowing translation speed of North Atlantic landfalling hurricanes and rainfall patterns, the geopotential height at 950 mb across the contiguous US on the tropical cyclone's date of landfall is analyzed for the full set of storms included in the study. Geopotential height is a vertical coordinate height that approximates the actual height of a pressure surface above mean-surface level. Lines drawn on a geopotential height map connect the locations on the map characterized by equivalent geopotential heights. A map of geopotential height anomalies depicts the deviations from the expected or average geopotential heights on a particular day. This variable is examined in conjunction with the precipitation fields on each date of landfall to assess the shape and location of each storm, enabling a more reliable and comprehensive analysis than would otherwise be possible if the latitude and longitude of the center of the storm were considered the most accurate measure of the storm's position. In this study, the Daily Intrinsic Pressure Level Geopotential Height from NOAA NCEP-NCAR CDAS-1 Reanalysis Project dataset is selected for the creation of geopotential height images for each landfalling date (Kalnay *et al*, 1996).

B. Analysis of Translation Speed Slowdown

To conduct the analysis of the slowdown in translation speed, a master spreadsheet of all of the relevant data for each North Atlantic tropical cyclone is first compiled and processed. In this spreadsheet, the year, month, date, and time of each TC observation is separated and filtered, and the latitude and longitude at each observation is carefully matched to its proper time of occurrence. Because the observations for hurricane position are processed with the corresponding wind speed at that point in time, the proper hurricane category according to the Saffir-Simpson hurricane classification scale (Tropical Depression, Tropical Storm, Category 1-5) could be used to categorize each storm into its appropriate category at each observation along its track. Thus, the storms incorporated into this clustering assessment include tropical depressions, tropical storms, and tropical cyclones, but these three classifications are collectively referred to as “hurricanes” or “tropical cyclones” in this study. This step allowed for a later analysis of trends in translation speed according to the category of each storm in the dataset.

After assembling a baseline spreadsheet with the processed data, the data could be inputted into ‘R’ programming software for a complete statistical analysis of translation speed (R, Core Development Team 2019). R is utilized to complete all statistical analyses pertaining to this study, as the program is well-suited to the manipulation, organization and processing of large data sets. Once the dataset is transferred from Excel to R, a loop function is applied to the data to calculate the minimum distance traveled by each storm during a moving 24-hour window throughout the storm’s development. Because the position data available for each track is recorded as a set of latitude-longitude coordinates, the Haversine formula is used to convert the difference between coordinates to the Euclidian distance in meters between two points on a sphere. Some pseudocode for the Haversine calculation is provided below for reference. The radius of the Earth is approximated as 6,371 meters in this analysis

```
#Defining difference in latitude and longitudes between two points

dLat = (lat2-lat1)
 dLon = (lon2-lon1)

#Calculation of Euclidian distance between two points

  a = sin(dLat/2) * sin(dLat/2) + cos(lat1) * cos(lat2) * sin(dLon/2) * sin(dLon/2)
  distance = 6371 * 2 * atan2(sqrt(a), sqrt(1-a))
```

With the minimum distance traveled in 24 hours for all storms calculated in a table, the minimum translation speed could then be analyzed through three distinct statistical analyses. A preliminary linear regression analysis, a k-means clustering analysis, and a k-nearest neighbor outlier detection test are all conducted to visualize temporal and spatial patterns in the translation speed of the North Atlantic hurricanes. The methodologies for these separate analyses are described below.

1. Linear Regression

A prefatory linear regression analysis is undertaken to assess the time series of minimum translation speeds associated with each TC. The statistical significance of the correlation is recorded and assessed. Based on a visual examination of the graph, a more complex statistical analysis is deemed necessary to dissect trends in the data.

2. Spatial and Temporal Analysis of Translation Speed

To gain a more nuanced understanding of the trends indicated by the preliminary analysis, the dataset of TCs is separated into three distinct time periods: 1851-1906, 1907-1960, 1961-2016. The latitude-longitude coordinate location of each storm while undergoing the slowest 24 hours of its track and the relative quantification of each storm's minimum speed is overlaid on a map of the North Atlantic basin. Three maps are produced to display the storm data for each subset of years. The purpose of this analysis is to enable both an assessment of the spatial characterization of the minimum translation speed over time and an evaluation of the changes to translation speed since 1851.

2. K-means Clustering Analysis of Translation Speed

A secondary statistical analysis is undertaken to classify the minimum translation speed of each TC according to five clusters determined through the supervised k-means clustering algorithm. K-means clustering is an organic methodology for grouping data that involves the identification of centroids that define the central points of each cluster and the subsequent allocation of specific data points to the nearest cluster. A methodology known as the elbow test is undertaken before clustering the translations speeds to identify the optimal number of clusters prior to the analysis. After the translation speeds are sorted into clusters, temporal trends are analyzed with respect to time to assess patterns in cluster membership since 1851.

3. *K-nearest neighbor Outlier Detection*

A final statistical test is devised to detect any significant outliers in translation speed. The k-nearest neighbor outlier detection test identifies outliers in datasets by comparing one data point to a specified number of neighboring points and examining the proximity of the points to one another according to some defined comparison metric. This analysis is pursued to identify any trends in the extremity of translation speeds in recent years.

C. Analysis of Storm-Related Precipitation at Landfall

1. Linear Regression Analysis

A linear regression examination is conducted for a subset of 181 landfalling storms contained within the larger dataset to examine trends in the maximum precipitation accumulation rate at landfall over time. The maximum precipitation within a 1 degree latitude-longitude box centered around the eye of each storm is recorded and processed. A time series is graphed with time in years on the x-axis, precipitation accumulation rate (in mm/day) on the y-axis, and linear regression line of best fit overlaid to illustrate the trend line.

2. Synoptic Precipitation Maps and Geopotential Height Anomaly Images

After assessing preliminary trends through a linear regression analysis, a program in 'R' is built to access and process reconstructed images of the rain fields and geopotential height anomaly fields over the contiguous United States on the dates of landfall for each storm. The precipitation and geopotential height field images are also generated for the three days preceding and three days following the date of landfall for each storm. The primary objective of this component of the analysis is to visually examine spatial trends in the precipitation fields over time rather than relying exclusively on the maximum precipitation accumulation rate as the sole metric of hurricane activity. This strategy is advised by a number of researchers, as hurricane rain fields are often asymmetrical and peculiar in shape (Zhou, 2018; Matyas, 2009; Matyas, 2017).

3. Hierarchal Clustering Analysis

The next step in this component of the analysis is a hierarchical clustering analysis of the spatial characterization of the main rain shields associated with each storm contained within the dataset. Hierarchal clustering is a clustering mechanism that organizes points into distinct clusters (much like the k-means clustering algorithm) and then presents the results as a dendrogram (tree diagram), in which each link in the diagram groups together elements from the group below. To conduct this analysis, the Livneh hydrometeorological dataset is downloaded for each date of landfall for 21 storms for which data is available in the dataset. Next, a code is generated to center the rain field around the latitude-longitude coordinates of the center of the storm to restrict the data to the immediate rain shield surrounding the storm. The resolution of the dataset is extremely fine (1/16 degree), so a 256 x 256-pixel square surrounding the storm center is processed for each date before the hierarchal clustering analysis is performed. A sample of this spatial image can be found in Figure 1.

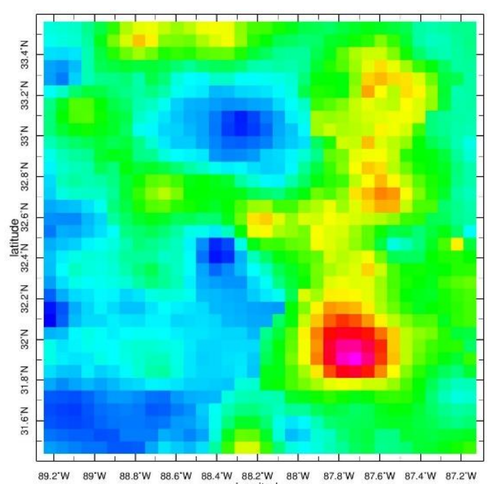

Figure 1. Sample spatial image of rain field for one date of landfall contained within dataset.

Results

A. Linear Regression

Figure 2 displays the time series of minimum translation speed averaged across all storms per year since 1851. The line of best fit for the data is illustrated and the linear regression equation is shown. The slope of the regression is tested for statistical significance and the returned p-value is equal to 0.0. The statistical significance analysis reveals that the correlation indicated between the two variables is due to a dependence between the variables rather than random chance. The shaded grey bands illustrate a 95% confidence interval, within which the most accurate estimate of the relationship between the predictor and response variable likely falls.

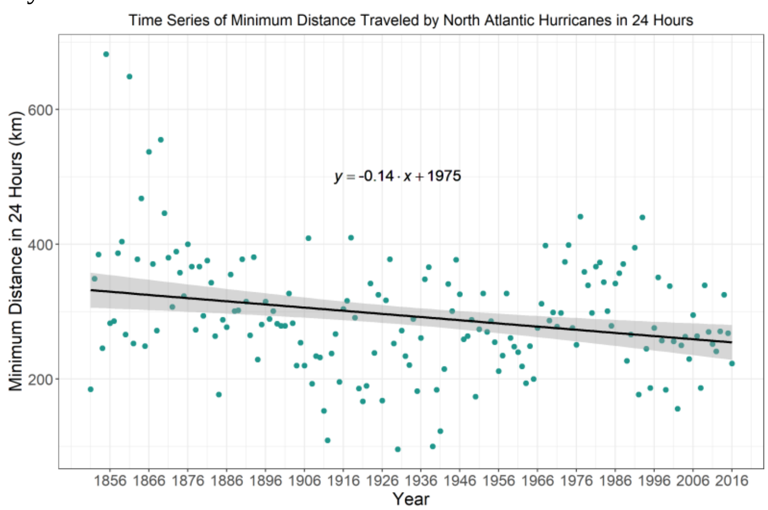

Figure 2. Linear regression calculated to quantify relationship between the minimum distance traveled by North Atlantic hurricanes in 24 hours (slowest translation speed) in km and time in years.

B. Analysis of Slowdown in Translation Speed

Figure 3 depict maps of the North Atlantic basin with the location of the slowest translation speed for each storm in the dataset denoted with a dot. Each dot is colored according to a logarithmic scale located to the right of the figure representing the relative value of that storm's minimum translation speed. The logarithmic scale emphasizes minute gradations in translation speed and reduces the overpowering influence of extreme outliers on the visual perception of the figure. Each map displays the tracks contained within a subset of the total number of years (1851-2016). Image **A** all tracks from 1851-1906. Image **B** depicts all tracks from 1907-1960. Image **C** depicts all tracks from 1961-2016. The separation of the tracks into three distinct groups allows for a visual assessment of the changes in translation speed with respect to both location and time. An analysis of these figures is discussed in more detail in the next section, but a preliminary visual observation indicates a clear increase in both the frequency of TCs and the number of TCs with slow minimum translation speeds.

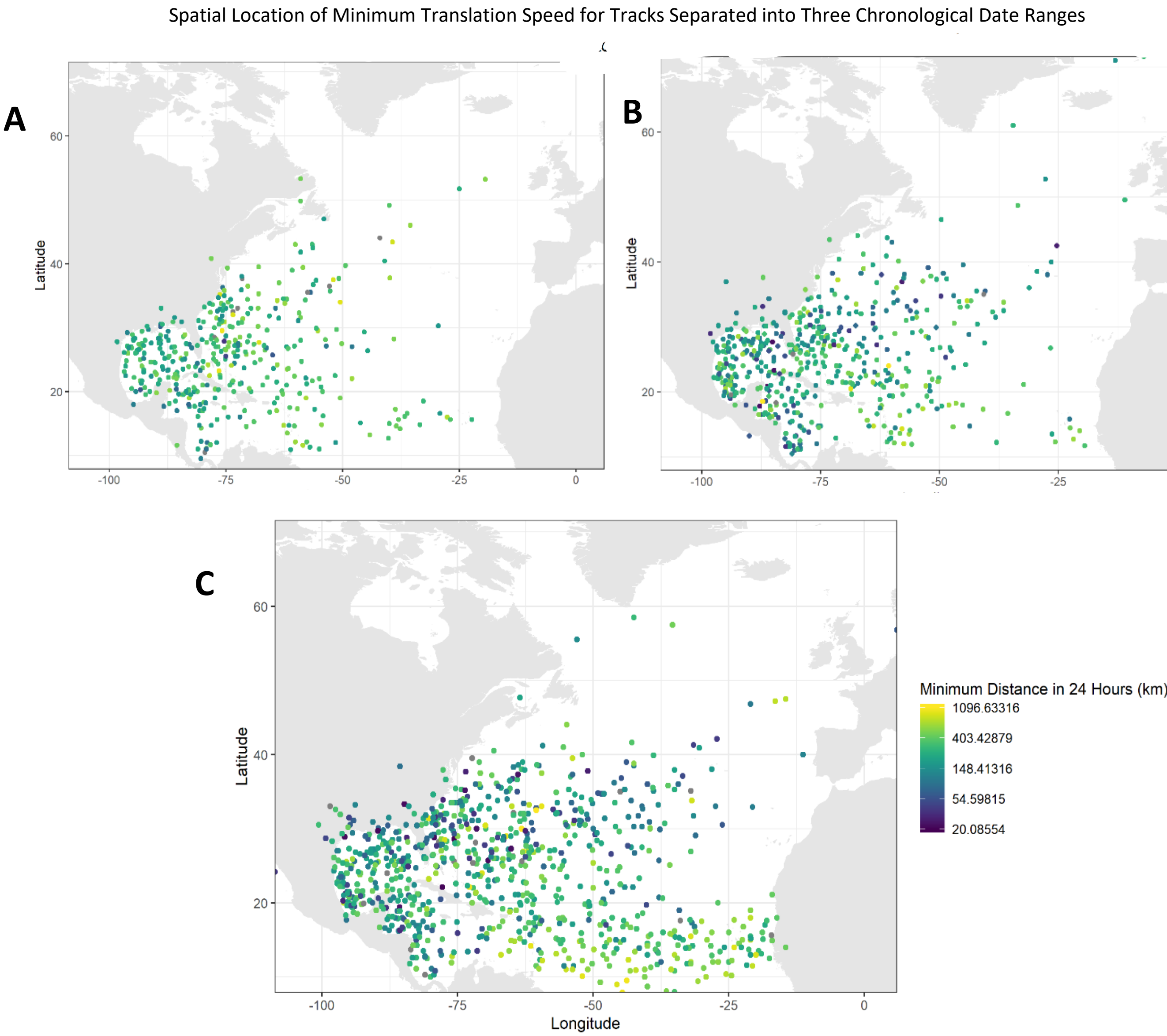

Figure 3. Maps of the North Atlantic Basin illustrating shifting patterns in the minimum distance traveled in 24 hours by North Atlantic hurricanes classified into three groups according to year of occurrence.

A series of additional figures are then produced in an attempt to visualize trends in minimum translation speed in three-dimensional space. The XYZ 3-D plot illustrated in **Figure 4** with a latitude-longitude representation of the North Atlantic Basin on the x- and y-axes and minimum distance plotted on the z-axis are designed, and each track is then plotted as a point colored according to a scale corresponding to the storm's year of occurrence. This procedure and result are explored further in the discussion, but this particular method of analysis is not pursued in greater detail due in large part to the challenge of processing such a large number of points in one figure.

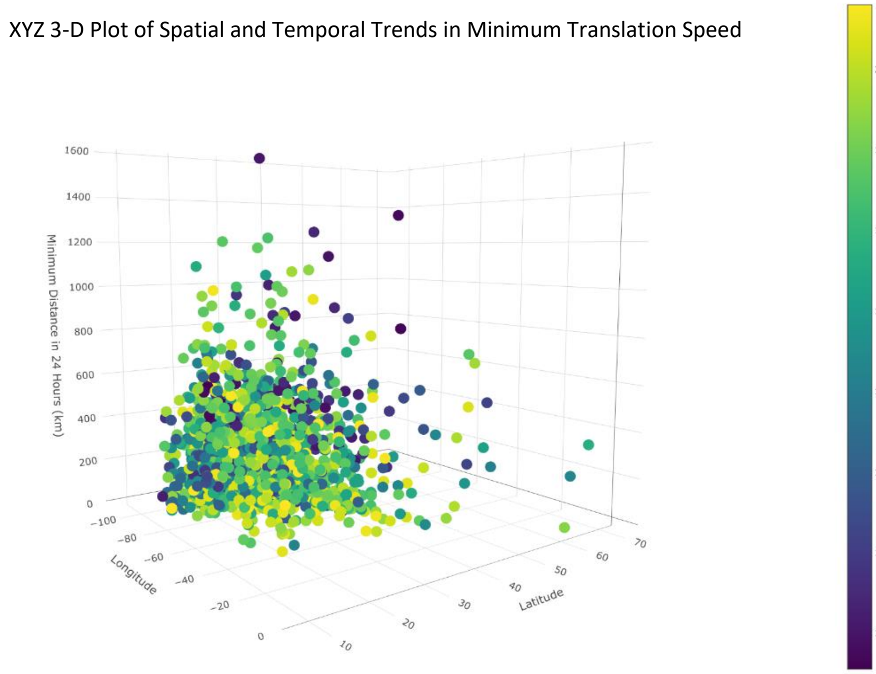

Figure 4. Sample XYZ 3-D plot produced to visualize spatial and temporal trends in the minimum distance traveled in 24 hours by North Atlantic TCs.

The final analysis directly related to minimum translation speed is a k-means clustering assessment. The five clusters generated to represent the dataset are shown in **Figure 5**, a time series of minimum distance in 24 hours (km) vs. time (years) colored according to a scale to differentiate between the five produced clusters. In order from least to greatest magnitude of minimum distance in 24 hours, the cluster classifications are: Cluster 3, Cluster 5, Cluster 2, Cluster 1, Cluster 4.

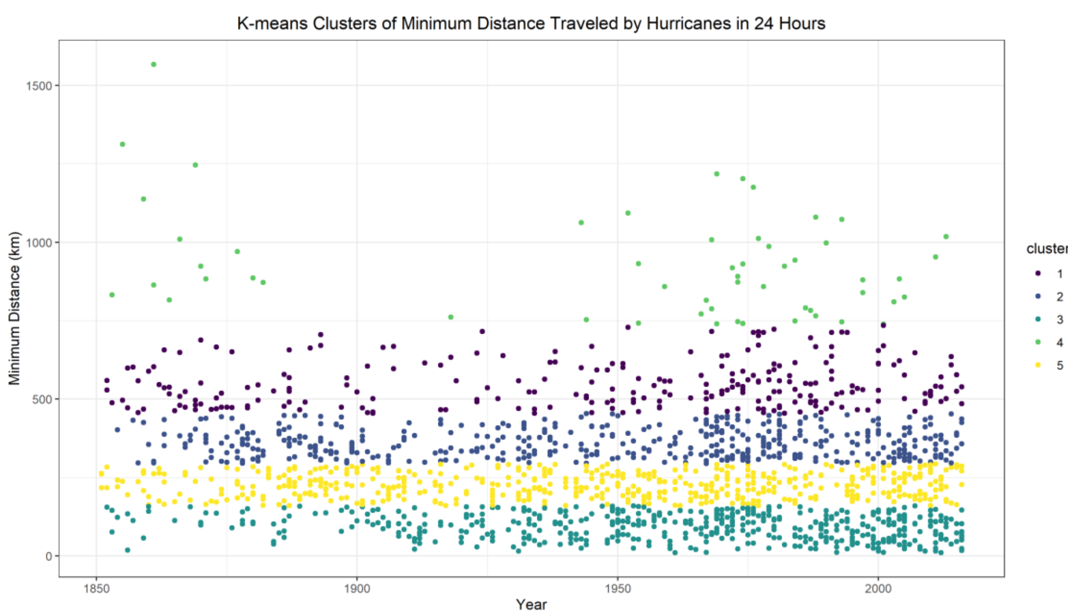

Figure 5. Time series of minimum distance in 24 hours vs. time with cluster membership displayed according to color scale on right.

According to the grouping of years utilized to separate the track dataset in **Figure 3** into three separate groups (1851-1906, 1907-1960, 1961-2016), a pie chart is produced to illustrate the percentage of total TCs belonging to Cluster 3 (the cluster containing the slowest minimum translation speed storms) during each year range. This pie chart (**Figure 6**) reveals that 27% of storms belonging to Cluster 3 occurred from 1851-2016, 26% of storms belonging to Cluster 3 occurred from 1907-1961, and 47% of storms belonging to Cluster 3 occurred from 1962-2016. Between 1962-2016 (the final 54 years analyzed in the study), nearly half of all of the slowest storms revealed by the k-means clustering analysis occurred.

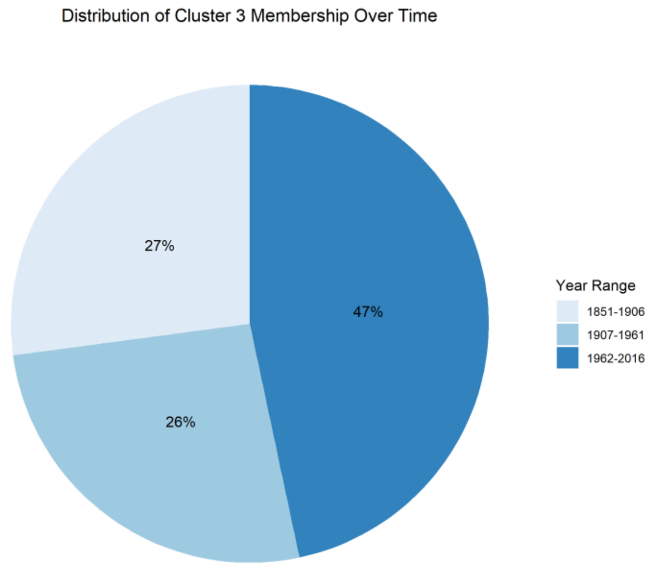

Figure 6. Pie chart displaying the distribution of Cluster 3 membership over time. Cluster 3 contains all North Atlantic TCS with the slowest minimum translation speeds identified in the dataset.

Figure 7 is a visual representation of a k-nearest neighbor outlier detection test designed to identify North Atlantic hurricanes with anomalous minimum distances in 24 hours. The statistical analysis reveals several outliers between 1851-2016, but all outliers isolated are storms with unusually high minimum distances rather than low minimum translation speeds. The results do not point to a significant temporal or spatial trend, and the timing of these highly anomalous storms appears randomized and unrelated to climatic shifts. The figure is organized so that time in years is indicated on the x-axis, latitude is displayed on the y-axis, and longitude is displayed on the z-axis.

\

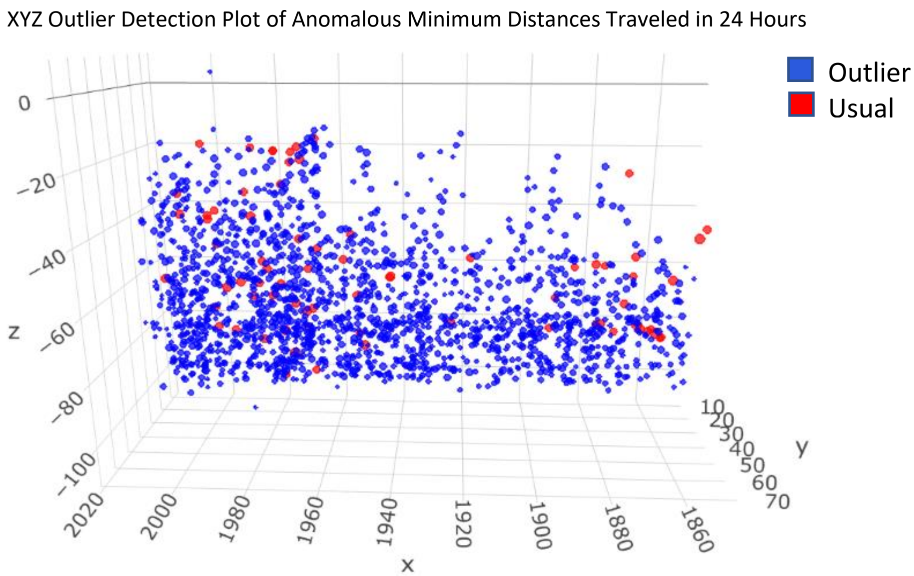

Figure 7. XYZ plot illustrating the results of a k-nearest neighbor outlier detection test. The outlier detection reveals a number of anomalous high minimum translation speeds but does not point to significant spatial or temporal trends in translation speed anomalies.

C. Analysis of Storm-Related Precipitation at Landfall

The second major component of the analysis involved an examination of the evolution of storm-related precipitation intensity at landfall. A cursory linear regression analysis (**Figure 8**) conducted on the set of 176 storms within the HURDAT2 dataset between 1950-2016 for which gridded landfall is available indicates that the precipitation accumulation rate is increasing at a rate of approximately 0.51 mm/day per year.

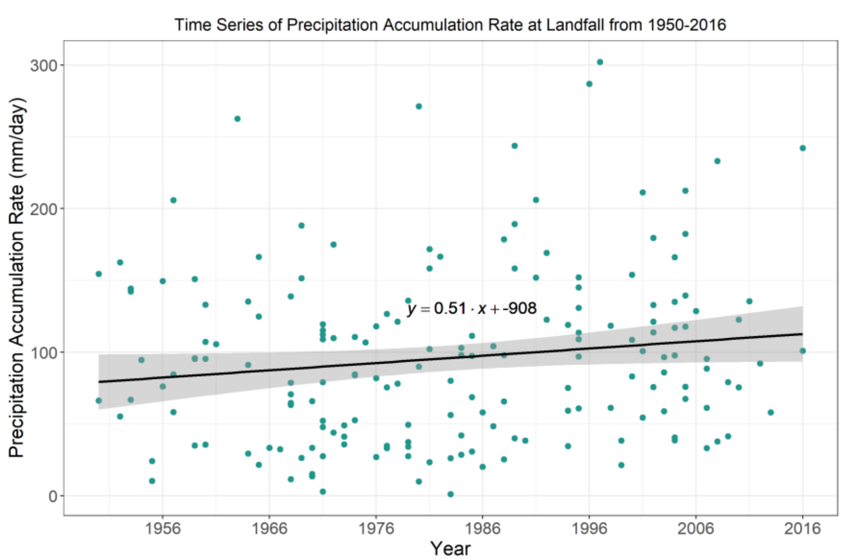

Figure 8. Time Series of Precipitation Accumulation Rate at Landfall from 1950-2016.

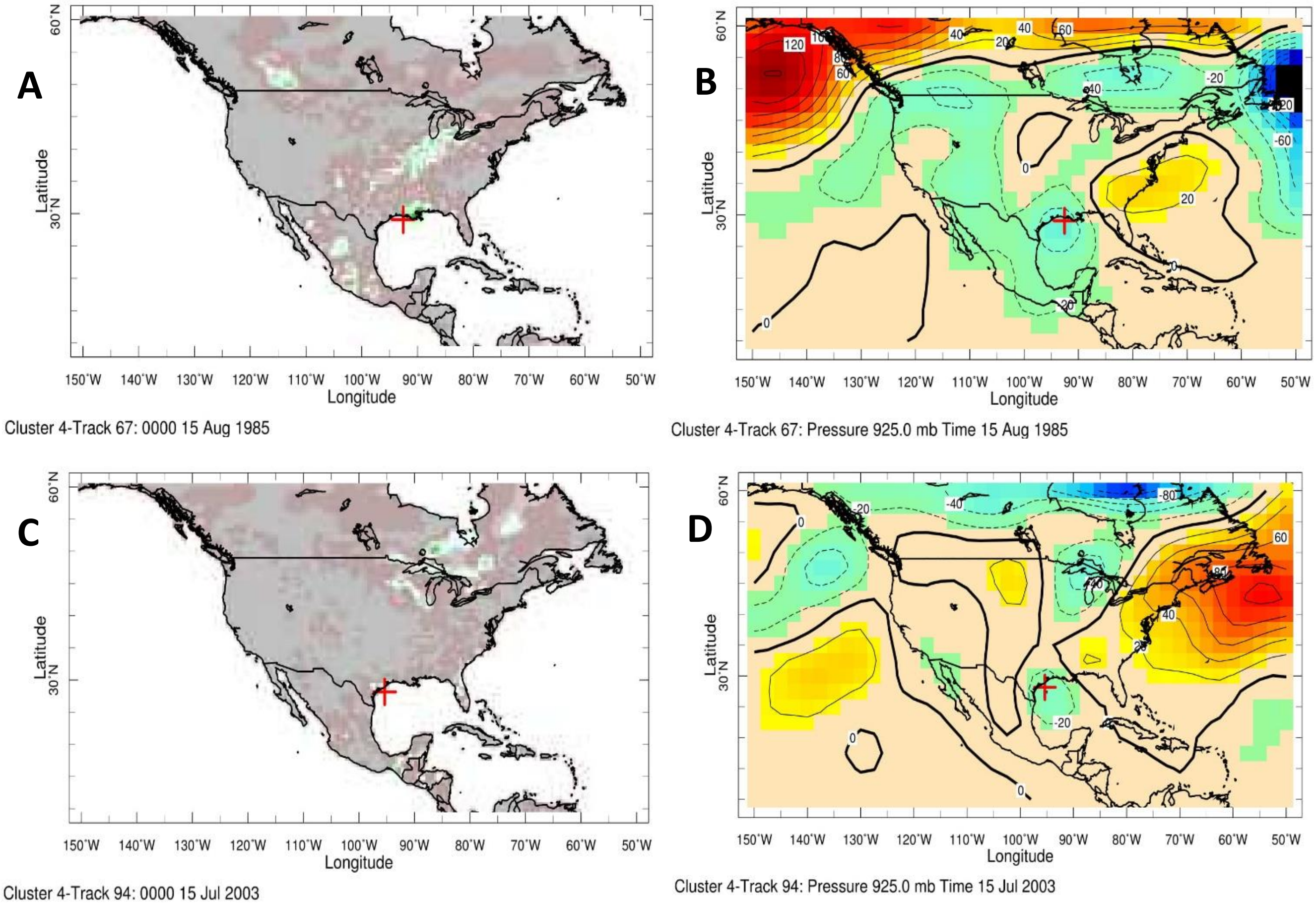

Figure 9. Sample synoptic rain field maps and geopotential height anomalies produced for two dates of landfall within the dataset. Selected dates are July 15th, 2003 August 15th, 1985.

After conducting the linear regression analysis and assessing the general precipitation intensity trend based on the maximum rainfall accumulation rate recorded within a 1 degree box centered around the eye of each storm, the individualized rain fields and geopotential height anomalies for the range of dates spanning three dates preceding and three days following the date of landfall were processed and analyzed. The 5000+ images were scrutinized to examine patterns in the distribution and extent of rainfall associated with each landfalling storm. Maximum rainfall accumulation rate on the landfall date enables some analysis of precipitation trends, but a visual assessment of rain fields and pressure systems offers a more complete examination of precipitation fields. **Figure 9** displays two sample figures produced during this portion of the analysis. A red cross denotes the location of the eye of the storm as indicated by its latitude-longitude coordinates in the HURDAT2 dataset. Maps **A** and **B** represent the precipitation fields and geopotential height anomalies on August 15th, 1985 and Maps **C** and **D** represent the precipitation fields and geopotential height anomalies on July 15th, 2003.

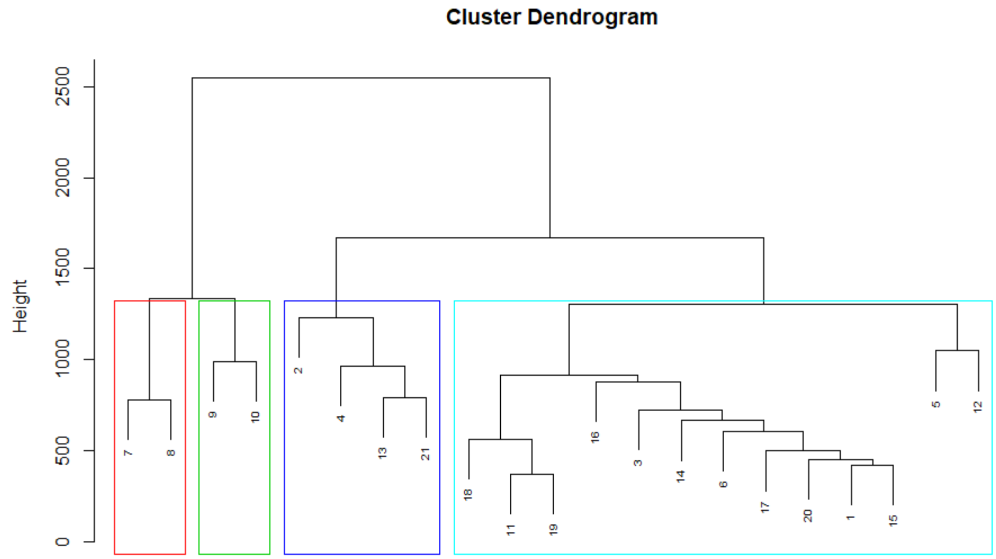

Figure 10. Hierarchal clustering dendrogram of spatial similarities in rainfall distribution and intensity between 1950-2011 for North Atlantic storms. Colored boxes emphasize the four main clusters identified by the statistical procedure.

The final component of the precipitation facet of the analysis involved the development of a cluster dendrogram illustrating the results of a hierarchal clustering assessment produced by computing the dissimilarities between the rain fields of storm tracks and classifying each track into a distinct group. The 21 storms within the dataset for which adequate data was available were analyzed in this manner. The track number of each storm shown in **Figure 10** refers to its chronological position within the dataset; thus, the track labeled ‘1’ is the earliest storm and the track labeled ‘21’ is the final storm from 1950-2016. The unsupervised hierarchal clustering analysis reveals a clear stratification of tracks, separating the earliest tracks within the dataset into three primary clusters and isolating nearly all recent storms into one group. A follow-up analysis of all spatial precipitation fields utilized for this analysis (a visual representation of this data can be found in **Figure 1**) reveals that the precipitation fields associated with recent storms are characterized by increasingly widespread intense rainfall accumulation rates and greater asymmetry in precipitation distribution. These results substantiate the preliminary conclusions concerning maximum precipitation accumulation rates indicated by the linear regression analysis while revealing similarities in the spatial composition of recent stagnant storms.

Discussion and Conclusions

In this investigation, a two-part analysis of North Atlantic TCs is undertaken to examine the relationship between the slowdown in translation speed and the intensification of storm precipitation. The minimum translation speed of 1,857 TCs over the timespan 1851-2016 is calculated, and this computation is then assessed through a linear regression analysis, a k-means clustering analysis, and a k-nearest neighbor outlier detection test. The results obtained through these three analyses are then linked to an assessment of storm-related rainfall intensification performed on precipitation accumulation data available for 185 storms within the dataset that made landfall between 1950-2011. A linear regression analysis of precipitation accumulation at landfall and a hierarchal clustering dendrogram are produced to examine preliminary trends in storm intensification at landfall and then classify tracks according to the spatial characteristics of each storm's local rain shield.

The linear regression analysis reveals that a weak but statistically significant correlation exists between time and the minimum translation speed of North Atlantic TCs. This conclusion supports the hypothesis that the minimum translation speed of North Atlantic TCs will decline over time, affirming the results of recent literature indicating that hurricane translation speed has decreased in not only the North Atlantic basin, but also the Indian Ocean basin and North Pacific basin (Kossin, 2018). Kossin investigates the slowdown in North Atlantic TC translation speed between 1950-2016, but the current study incorporates an expanded dataset of tracks from 1851-2016, enabling a more complete analysis of trends in the North Atlantic from the earliest available HURDAT2 track data. The results of this analysis indicate a steady decrease in minimum translation speed over time, but the North Atlantic slowdown is accompanied by a rise in the frequency of North Atlantic hurricanes, a coupling effect that may exacerbate the implications of TC slowdown and heighten the vulnerability of coastal regions to the flooding damages associated with major storms.

The conclusion that the frequency of North Atlantic hurricanes has increased since 1851, particularly between 1962-2016, is substantiated by a number of research studies, but intrinsic limitations in the HURDAT2 dataset must be acknowledged when considering this finding. As discussed in the methodology section, reconnaissance aircraft data collection was implemented into hurricane documentation in 1944 and the integration of satellite radar images into the dataset closely followed. Pre-1944, the HURDAT2 dataset was compiled primarily using weather station observations and ship records, and the inherent inconsistencies and inaccuracies in the full dataset are well-acknowledged (Torn and Snyder, 2012). Despite the limitations in the HURDAT2 dataset, the increase in frequency of North Atlantic hurricanes determined by this study warrants attention when considering the interconnected implications of increasingly active hurricane activity in the North Atlantic.

This increasingly active hurricane activity in the North Atlantic hurricanes is often speculated to be the direct result of anthropogenic warming, a claim explored in the introductory section of this study that is now supported by the results of the investigation. The weakening of the mid-latitude circulation due to increased global temperatures is considered the impetus for the reduced strength of the prevailing wind patterns responsible for directing North Atlantic hurricanes, a relationship that could explain the stalling patterns evident in recent storms (Screen and Simmons, 2014; Kossin, 2018). However, recent literature has explored the claim that the stalling of recent TCs cannot necessarily be attributed exclusively to human-induced climate change. A study published by Hall and Kossin in 2019 stipulated that low frequency natural variability must also be considered in assessments of the cause of this observed pattern. The impacts of regular climatic cycles, such as El Niño Southern Oscillation and the Atlantic Multidecadal Oscillation (a mode of climate variability defined by regular fluctuations in North Atlantic sea surface temperature), cannot be discounted. In any case, the recent increases in TC stalling and the high potential for subsequent precipitation-related damages pose a serious threat to the safety and stability of coastal populations.

The links between anthropogenic warming, translation speed, and precipitation intensity are not always direct, but the results of this study support the hypothesis that a decline in translation speed is likely accompanied by a rise in precipitation accumulation rate at landfall and an increase in flooding-related damages. The trend illustrated in illustrates the weak but statistically significant positive correlation between time and precipitation accumulation rate of landfalling hurricanes between 1950-2016. This conclusion is supported by Hall and Kossin's 2019 study, which contends that the annual-mean rainfall from stalling TCs on the U.S. has risen significantly due to the rising stalling frequency, and that the increased stalling can be attributed to a reduction in TC translation speed and a trend toward large and abrupt deviations in direction. The dendrogram also reveals that recent storms are far more comparable in terms of their spatial rain field composition, with precipitation fields becoming increasingly asymmetric and rain field intensity becoming more widespread. The synoptic rain field images produced in the visual observation component of the analysis reinforce this conclusion.

The limitations of the dataset must once again be taken into consideration when assessing this result. Ideally, the precipitation associated with each track in the initial HURDAT2 dataset at every step in its development could be analyzed in the context of its translation speed at that point. Unfortunately, a global daily precipitation dataset containing oceanic rainfall does not presently exist; thus, studies of this nature are limited to interpolated precipitation estimates over land in the contiguous United States. The quality of interpolated precipitation datasets is steadily improving, and increasingly fine resolution datasets are regularly released, but early measurements of TC-related rainfall contain some inaccuracies, even in the recently released Livneh hydrometeorological dataset utilized in this study.

Continued research in this area is promising, however. Investigation of the impacts of anthropogenic warming on North Atlantic TCs and the methodology that can be used to accurately model these complex relationships will improve long-term hurricane prediction and improve societal resilience to the imminent threat of climate change. In an era dominated by the ever-increasing intensity and frequency of North Atlantic hurricanes, an understanding of the links between translation speed, precipitation intensity, and anthropogenic warming is of paramount importance.

REFERENCES

Alemany, S., Beltran, J., Perez, A., & Ganzfried, S. (2018). Predicting Hurricane Trajectories using a Recurrent Neural Network. *ArXiv:1802.02548 [Physics, Stat]*. Retrieved from http://arxiv.org/abs/1802.02548

Atallah, E., Bosart, L. F., & Aiyyer, A. R. (2007). Precipitation Distribution Associated with Landfalling Tropical Cyclones over the Eastern United States. *Monthly Weather Review*, *135*(6), 2185–2206. https://doi.org/10.1175/MWR3382.1

Chen, H. (2015). Downstream development of baroclinic waves in the midlatitude jet induced by extratropical transition: A case study. *Advances in Atmospheric Sciences*, *32*(4), 528–540. https://doi.org/10.1007/s00376-014-3263-8

Chen, M., W. Shi, P. Xie, V. B. S. Silva, V E. Kousky, R. Wayne Higgins, and J. E. Janowiak (2008), Assessing objective techniques for gauge-based analyses of global daily precipitation, J. Geophys. Res., 113, D04110, doi:10.1029/2007JD009132.

Chen, M., P. Xie, and Co-authors (2008), CPC Unified Gauge-based Analysis of Global Daily Precipitation, Western Pacific Geophysics Meeting, Cairns, Australia, 29 July - 1 August, 2008

Coumou, D., Lehmann, J., & Beckmann, J. (2015). Climate change. The weakening summer circulation in the Northern Hemisphere mid-latitudes. *Science (New York, N.Y.)*, *348*. https://doi.org/10.1126/science.1261768

data: Expert Mode. (n.d.). Retrieved August 23, 2019, from http://iridl.ldeo.columbia.edu/SOURCES/.NOAA/.NCEP/.CPC/.UNIFIED_PRCP/.GAUGE_BASED/.GLOBAL/.v1p0/.RETRO/.rain/X/-150/-50/RANGE/Y/10/60/RANGE/SOURCES/.NOAA/.NCEP/.CPC/.UNIFIED_PRCP/.GAUGE_BASED/.GLOBAL/.v1p0/.REALTIME/.rain/X/-150/-50/RANGE/Y/10/60/RANGE/appendstream/prcp_fraction_colors/DATA/0/80/RANGE//color_smoothing/null/def/#expert

Estimating Tropical Cyclone Intensity by Satellite Imagery Utilizing Convolutional Neural Networks: Weather and Forecasting: Vol 34, No 2. (n.d.). Retrieved August 6, 2019, from https://journals.ametsoc.org/doi/abs/10.1175/WAF-D-18-0136.1

Finocchio, P. M., Doyle, J. D., Finocchio, P. M., & Doyle, J. D. (2019). How the Speed and Latitude of the Jet Stream Affect the Downstream Response to Recurving Tropical Cyclones. *Monthly Weather Review*. https://doi.org/10.1175/MWR-D-19-0049.1

Galarneau, T. J., Bosart, L. F., & Schumacher, R. S. (2010). Predecessor Rain Events ahead of Tropical Cyclones. *Monthly Weather Review*, *138*(8), 3272–3297. https://doi.org/10.1175/2010MWR3243.1

Global Unified Precipitation Gridded Dataset. (n.d.). Retrieved July 26, 2019, from http://iridl.ldeo.columbia.edu/SOURCES/.NOAA/.NCEP/.CPC/.UNIFIED_PRCP/.GAUGE_BASED/.GLOBAL/.v1p0/.RETRO/.rain/X/-150/-50/RANGE/Y/10/60/RANGE/SOURCES/.NOAA/.NCEP/.CPC/.UNIFIED_PRCP/.GAUGE_BASED/.GLOBAL/.v1p0/.REALTIME/.rain/X/-150/-50/RANGE/Y/10/60/RANGE/appendstream/index.html#info

Grams, C. M., & Archambault, H. M. (2016). The Key Role of Diabatic Outflow in Amplifying the Midlatitude Flow: A Representative Case Study of Weather Systems Surrounding Western North Pacific Extratropical Transition. *Monthly Weather Review*, *144*(10), 3847–3869. https://doi.org/10.1175/MWR-D-15-0419.1

Hall and Kossin—2019—Hurricane stalling along the North American coast .pdf. (n.d.). Retrieved from https://www.nature.com/articles/s41612-019-0074-8.pdf

Hall, T. M., & Kossin, J. P. (2019). Hurricane stalling along the North American coast and implications for rainfall. *Npj Climate and Atmospheric Science*, *2*(1), 17. https://doi.org/10.1038/s41612-019-0074-8

Hanley, D., Molinari, J., & Keyser, D. (2001). A Composite Study of the Interactions between Tropical Cyclones and Upper-Tropospheric Troughs. *Monthly Weather Review*, *129*(10), 2570–2584. https://doi.org/10.1175/1520-0493(2001)129<2570:ACSOTI>2.0.CO;2

Hodyss, D., & Hendricks, E. (2010). The Resonant Excitation of Baroclinic Waves by the Divergent Circulation of Recurving Tropical Cyclones. *Journal of the Atmospheric Sciences*, *67*(11), 3600–3616. https://doi.org/10.1175/2010JAS3459.1

Lachmy, O., & Harnik, N. (2016). Wave and Jet Maintenance in Different Flow Regimes. *Journal of the Atmospheric Sciences*, *73*(6), 2465–2484. https://doi.org/10.1175/JAS-D-15-0321.1

Liu, M., & Smith, J. A. (2016). Extreme Rainfall from Landfalling Tropical Cyclones in the Eastern United States: Hurricane Irene (2011). *Journal of Hydrometeorology*, *17*(11), 2883–2904. https://doi.org/10.1175/JHM-D-16-0072.1

Lunga, D., & Ersoy, O. (2011). Spherical Nearest Neighbor Classification: Application to Hyperspectral Data. In P. Perner (Ed.), *Machine Learning and Data Mining in Pattern Recognition* (Vol. 6871, pp. 170–184). https://doi.org/10.1007/978-3-642-23199-5_13

Matsuoka, D., Nakano, M., Sugiyama, D., & Uchida, S. (2018). Deep learning approach for detecting tropical cyclones and their precursors in the simulation by a cloud-resolving global nonhydrostatic atmospheric model. *Progress in Earth and Planetary Science*, *5*(1), 80. https://doi.org/10.1186/s40645-018-0245-y

Matyas, C. J. (2010). Associations between the size of hurricane rain fields at landfall and their surrounding environments. *Meteorology and Atmospheric Physics; Wien*, *106*(3–4), 135–148. http://dx.doi.org/10.1007/s00703-009-0056-1

Matyas, C. J. (2013). Processes Influencing Rain-Field Growth and Decay after Tropical Cyclone Landfall in the United States. *Journal of Applied Meteorology and Climatology*, *52*(5), 1085–1096. Retrieved from JSTOR.

Matyas, C. J. (2017). Comparing the Spatial Patterns of Rainfall and Atmospheric Moisture among Tropical Cyclones Having a Track Similar to Hurricane Irene (2011). *Atmosphere*, *8*(9), 165. https://doi.org/10.3390/atmos8090165

Mei, W., Pasquero, C., & Primeau, F. (2012). The effect of translation speed upon the intensity of tropical cyclones over the tropical ocean. *Geophysical Research Letters*, *39*(7). https://doi.org/10.1029/2011GL050765

Nakamura, J., Lall, U., Kushnir, Y., & Rajagopalan, B. (2015). HITS: Hurricane Intensity and Track Simulator with North Atlantic Ocean Applications for Risk Assessment. *Journal of Applied Meteorology and Climatology*, *54*(7), 1620–1636. https://doi.org/10.1175/JAMC-D-14-0141.1

Nakamura, Jennifer, Lall, U., Kushnir, Y., & Camargo, S. J. (2009). Classifying North Atlantic Tropical Cyclone Tracks by Mass Moments. *Journal of Climate*, *22*(20), 5481–5494. https://doi.org/10.1175/2009JCLI2828.1

Pohorsky, R., Röthlisberger, M., Grams, C. M., Riboldi, J., & Martius, O. (2019). The Climatological Impact of Recurving North Atlantic Tropical Cyclones on Downstream Extreme Precipitation Events. *Monthly Weather Review*, *147*(5), 1513–1532. https://doi.org/10.1175/MWR-D-18-0195.1

Rasp, S., & Lerch, S. (2018). Neural Networks for Postprocessing Ensemble Weather Forecasts. *Monthly Weather Review*, *146*(11), 3885–3900. https://doi.org/10.1175/MWR-D-18-0187.1

Sahoo, B., & Bhaskaran, P. K. (2019). Prediction of storm surge and coastal inundation using Artificial Neural Network – A case study for 1999 Odisha Super Cyclone. *Weather and Climate Extremes*, *23*, 100196. https://doi.org/10.1016/j.wace.2019.100196

Schumacher, R. S., Galarneau, T. J., & Bosart, L. F. (2010). Distant Effects of a Recurving Tropical Cyclone on Rainfall in a Midlatitude Convective System: A High-Impact Predecessor Rain Event. *Monthly Weather Review*, *139*(2), 650–667. https://doi.org/10.1175/2010MWR3453.1

Scoccimarro, E., Gualdi, S., Villarini, G., Vecchi, G. A., Zhao, M., Walsh, K., & Navarra, A. (2014). Intense Precipitation Events Associated with Landfalling Tropical Cyclones in Response to a Warmer Climate

and Increased CO_2. *Journal of Climate*, *27*(12), 4642–4654. Retrieved from JSTOR.
Villarini, G., Smith, J. A., Baeck, M. L., Marchok, T., & Vecchi, G. A. (2011). Characterization of rainfall distribution and flooding associated with U.S. landfalling tropical cyclones: Analyses of Hurricanes Frances, Ivan, and Jeanne (2004). *Journal of Geophysical Research: Atmospheres*. https://doi.org/10.1029/2011JD016175
Zhou, Y., & Matyas, C. J. (2018). Spatial Characteristics of Rain Fields Associated with Tropical Cyclones Landfalling over the Western Gulf of Mexico and Caribbean Sea. *Journal of Applied Meteorology and Climatology*, *57*(8), 1711–1727. https://doi.org/10.1175/JAMC-D-18-0034.1